

## COMMUNICATION

[View Article Online](#)  
[View Journal](#) | [View Issue](#)



Cite this: *Dalton Trans.*, 2024, **53**, 18462

Received 10th September 2024,  
Accepted 22nd October 2024

DOI: 10.1039/d4dt02588a  
[rsc.li/dalton](http://rsc.li/dalton)

## Modification of cobalt bis(dicarbollide) ions with nitrile groups on carbon atoms: a unique low-temperature skeletal rearrangement due to the specific electron-donor character of CN substitution†

Ece Zeynep Tüzün, <sup>a,b</sup> Drahomír Hnyk, <sup>a</sup> Dmytro Bavol, <sup>a</sup> Miroslava Litecká, <sup>a</sup> Jindřich Fanfrlík<sup>c</sup> and Bohumír Gruner <sup>a,\*</sup>

Herein, we report on the synthesis and stereochemistry of mono- and isomeric dinitrile derivatives of  $[(1,2\text{-C}_2\text{B}_9\text{H}_{11})_2\text{-}3,3'\text{-Co}]^-$  ions. The shape and electronic properties of CN groups can apparently surmount the strain associated with the substitution of two vicinal carbon positions. Owing to electron donation to the cage, this results in a substituent-induced rearrangement of one of the carbon atoms to the upper pentagonal ring. The molecular structure of this isomer was confirmed using sc-XRD and DFT chemical computations.

A bis-icosahedral cobalt bis(1,2-dicarbollide)(1-) anion,<sup>1–3</sup>  $[(1,2\text{-C}_2\text{B}_9\text{H}_{11})_2\text{-}3,3'\text{-Co}]^-$  (**1**<sup>–</sup>), is characterized by fully occupied orbitals of the metal with 18 e<sup>–</sup>, aromaticity,<sup>4</sup> very robust chemical, thermal and radiation stability, low-nucleophilic properties,<sup>5</sup> and its behaviour like stealth amphiphile<sup>6</sup> or superchaotropic<sup>7</sup> in aqueous solutions. It has attracted considerable attention as an anionic scaffold for various emerging applications.

Considering medicinal chemistry<sup>8</sup> on which we currently focus, the parent ion has been proven to have relatively low toxicity and can easily penetrate cells.<sup>9,10</sup> The ion forms supramolecular assemblies and<sup>11</sup> vesicles,<sup>12</sup> interacts strongly with proteins,<sup>13</sup> can serve as a delivery agent for BNCT,<sup>14,15</sup> transport cationic peptides through cell membranes,<sup>7</sup> enhance the antibiotic action of some drugs<sup>16</sup> and can specifically inhibit the HIV-Protease enzyme with an IC<sub>50</sub> value of 1  $\mu\text{mol}$ .<sup>9</sup>

The anion **1**<sup>–</sup> can be readily modified on the B(8) vertex through electrophile-induced nucleophilic substitution (EINS) pathways.<sup>3,17</sup> With this advantage, the nucleophile is a cyclic ether that produces species containing an oxonium atom.<sup>17</sup> Such rings can be easily cleaved with a broad range of nucleophilic reagents.<sup>18</sup> This method has shown high potential in the medicinal chemistry of ion **1**<sup>–</sup> and for the development of polymers,<sup>19</sup> dendrimers<sup>20,21</sup> and materials,<sup>22</sup> although at the expense of limited possibilities of modifying the length of the linker and stereochemistry.<sup>1</sup>

Considering the experimental difficulties in the initial stages of development, functionalization of the ion **1**<sup>–</sup> on carbon atoms has only recently emerged as a versatile method for creating anionic building blocks applicable in the rational design of biologically active boron-cluster compounds for various therapeutic targets, such as enzyme inhibitors, antibiotics, and cytotoxic species, or in the construction of advanced molecular architectures and materials.<sup>2,8</sup> The use of the latter approach allows for the introduction of different dipole moments and possibilities of fine-tuning the proton affinity of protable groups (OH, NH<sub>3</sub>, COOH, *etc.*) as well as the distance between the functional group and the cage by a one atom increment. These may be the critical factors in attaining optimal interactions with the active site of enzymes such as carbonic anhydrase IX.<sup>23</sup> Considering disubstitutions, carbon functionalization offers, in principle, three isomers with different space orientations of groups, denoted previously as chiral *racemic*-, and symmetric *meso*- and *vicinal*-forms. *Racemic* isomers, which are characterized by the largest separation between substituents, are usually the most abundant species resulting from reactions of the lithiated anion **1**<sup>–</sup> with electrophiles. In contrast, *vicinal* isomers have not been isolated from direct reactions yet, although their presence in low ratios has been observed through HPLC in several reaction mixtures.<sup>2</sup>

Compounds substituted with a nitrile group belong to the most valuable reagents and building blocks in organic chem-

<sup>a</sup>Institute of Inorganic Chemistry, Czech Academy of Sciences, 25068 Řež, Czech Republic. E-mail: gruner@iic.cas.cz

<sup>b</sup>Dpt. of Inorganic Chemistry, Charles University, Hlavova 2030, 12843 Prague 2, Czech Republic

<sup>c</sup>Institute of Organic Chemistry and Biochemistry, Czech Academy of Sciences, 166 10 Prague 6, Czech Republic

† Electronic supplementary information (ESI) available: Additional experimental details, crystallographic tables, and additional supporting figures. CCDC 2370281 and 2370282. For ESI and crystallographic data in CIF or other electronic format see DOI: <https://doi.org/10.1039/d4dt02588a>



istry because of their smooth interconversions to carboxylates, amines, and heterocycles *via* cycloaddition and other reactions. Considering synthesis, it is known that the direct introduction of functional groups on the C-atoms of ion  $1^-$  (with no linker) may present certain difficulties connected with shielding of the reaction sites due to the steric and electronic effects of the bulky anionic cage. Also, the physicochemical properties of the resulting compounds can be significantly altered, as was recently exemplified by the substitution with  $-\text{NH}_2$  and  $-\text{N}_3$  groups.<sup>24</sup> Thus, although nitriles attached *via* an alkane linker could be easily prepared starting from the respective alkyl methylsulfonyl esters,<sup>25</sup> synthesis of the first member of the series was unsuccessful. Indeed, our previous attempts to prepare the target nitriles using cyanogen bromide or trimethylsilyl cyanide resulted in high-yield bromination<sup>25</sup> or silylation of the cage carbon(s) instead, due to the ambiguous behaviour of the bromine or silylum ion under the applied reaction conditions. However, we show here that low-temperature reaction of the lithiated cage with toluene sulfonyl cyanide (TsCN) led to the smooth formation of the respective nitriles with the general formulae  $[(1\text{-CN-1,2-C}_2\text{B}_9\text{H}_{10})(1',2'\text{-C}_2\text{B}_9\text{H}_{11})_3,3'\text{-Co(III)}]^-$  ( $2^-$ ) and  $[(\text{CN-C}_2\text{B}_9\text{H}_{10})_2\text{-Co(III)}]^-$  ( $3^-$ ). As evidenced by HPLC analyses and mass spectroscopy of the reaction mixtures, the reaction did not go to full completion and produced equilibrium mixtures of the parent anion with the corresponding nitriles, even when high ratios of ion  $1^-$  to the base and TsCN of 1:3.0 were used. Starting from a ratio of 1:1.50, also several isomeric trisubstituted products were formed in low quantities; however, these could not be isolated in sufficient purity due to their limited hydrolytic stability during RP chromatography in an aqueous mobile phase, which was essential for separation of the mixture of anionic products.

The main products were isolated using extraction into diethyl ether followed by separation with flash chromatography on C18 RP Büchi columns. The monosubstituted compound  $2^-$  was isolated as the main product from the reactions carried out in ratios up to 1:1.75 and was fully characterized by a combination of HPLC, HRMS, and NMR techniques (see in ESI†). Concerning the disubstituted compounds  $3^-$ , the presence of several isomers was observed in the reaction mixture. However, only two main products, stable towards air and moisture, could be isolated. The first one, characterized using spectral methods and XRD corresponded to the red *rac*-isomer with the formula  $[(1,1'\text{-CN-1,2-C}_2\text{B}_9\text{H}_{10})_2\text{-3,3'\text{-Co(III)}]}^-$  ( $3\text{a}^-$ ) (see Fig. 1 and Scheme 1), which was apparently the most thermodynamically stable species out of the three “conventional” isomers. This formed as the main product when the cooling and stirring of the reaction mixture to  $-82^\circ\text{C}$  was continued for at least for 3 h. This compound was separated and characterized using analytical HPLC, HRMS, NMR, and sc-XRD (see Fig. 1 and the ESI†). The ratio of the second species increased upon faster warming up the reaction mixture and prevailed when the cooling bath was completely removed after 30 min after the addition of TsCN. However, the patterns observed in the  $^{11}\text{B}$  NMR spectrum of this isomer did not

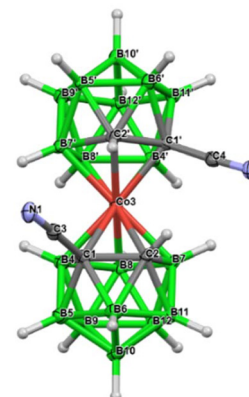
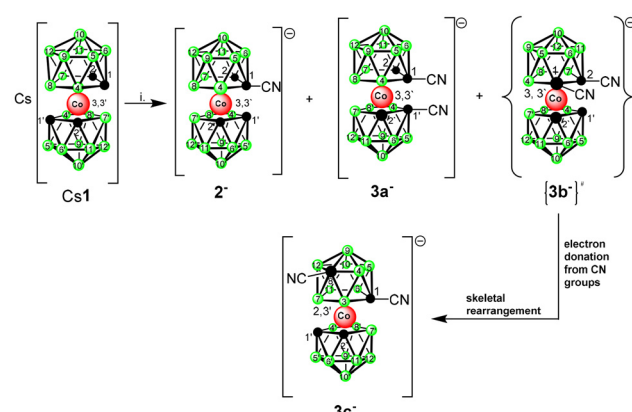


Fig. 1 Crystal structure of the anion *rac*- $3\text{a}^-$ ; the  $\text{Me}_4\text{N}^+$  cation is omitted for clarity (ORTEP view, ellipsoids are drawn with 40% probability). The structural parameters and selected interatomic distances and angles are presented and discussed in the Crystallographic part in the ESI.†



Scheme 1 Synthesis of nitriles; conditions: i.  $\text{BuLi}$ ,  $\text{DME}$ ,  $-82^\circ\text{C}$ , then  $\text{TsCN}$  in  $\text{DME}$  at  $-82^\circ\text{C}$ , ratios of  $1^-$ :reagents, from 1:1.5 to 1:3.0, 12 h stirring from 30 min to 3 h,  $-82^\circ\text{C}$  to  $20^\circ\text{C}$  during 12 h, extraction, RP chromatography. \*Assumed intermediate isomer.

match with the expected *meso*-isomer. Instead, the  $^{11}\text{B}$  NMR spectrum contained 13 distinguishable boron signals, of which one part corresponding to the unsubstituted dicarbolide ligand matched closely with the pattern for the parent ion  $1^-$ , showing boron signals with intensities of 1:1:2:2:2:1. The pattern of the second ligand was completely asymmetric, corresponding to 9 signals of intensity 1, among which, however, five peaks overlapped by coincidence. Two distinguishable CH signals could be seen in the  $^1\text{H}$  NMR spectrum; however, only one signal could be observed for the CH and  $\text{C}_{\text{cage}}$  carbons in the  $^{13}\text{C}$  NMR analysis and two signals for CN groups (see the ESI†).

The structure of this species was unambiguously confirmed by X-ray diffraction analysis performed on crystals isolated from two independent runs, for certainty (Fig. 2). Curiously, the sc-XRD structure showed the migration of one of the substituted skeletal carbon atoms to the upper pentagon of the



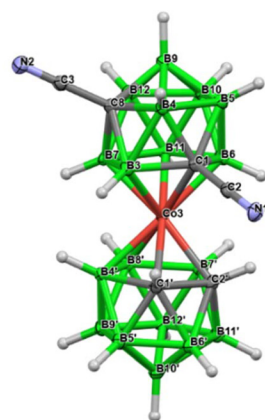


**Fig. 2** Crystal structure of the anion  $3c^-$ ; the cation is omitted for clarity (ORTEP view, ellipsoids are drawn with 40% probability). The structural parameters and selected interatomic distances and angles are given and discussed in the Crystallographic part in the ESI.†

dicarbollide ion, which was non-adjacent to Co(III). Only one rearranged isomer corresponding to the formula  $[(1,8\text{-CN}_2\text{-1,2-}C_2\text{B}_9\text{H}_9)(1',2'\text{-C}_2\text{B}_9\text{H}_{11})\text{-2,3'-Co(III)}]^-$  ( $3c^-$ ) could be seen; therefore the rearrangement was highly stereospecific. According to HPLC analysis, the rearrangement proceeded during warming up the reaction mixture from  $-82\text{ }^\circ\text{C}$  up to room temperature. Concerning the ionic full-sandwich metal bis(dicarbollides), such a low-temperature pathway has no precedent. Only the 1,7-isomer of cobalt bis(dicarbollide) is known, in which both carbons remain adjacent to the Co(III) atom. This is typically prepared by cobalt insertion into the  $[7,9\text{-C}_2\text{B}_9\text{H}_{12}]^-$  ion and eventually is also accessible *via* thermal rearrangement in a high-temperature interval starting at  $346\text{ }^\circ\text{C}$ .<sup>3,26</sup> The closely related thermal isomerization of the mixed  $[3\text{-CpCo-1,2-}C_2\text{B}_9\text{H}_{11}]$  sandwich was studied in more detail in the range  $400\text{--}700\text{ }^\circ\text{C}$ . Depending on the temperature, variable ratios of several isomers were formed, inclusive of the 1,8-species.<sup>27,28</sup> Therefore, the introduction of two linear-shaped and electron-rich nitrile groups on one ligand of the cage had unexpectedly important consequences. Our considerations, supported by theoretical computations performed at the SMD( $\text{Et}_2\text{O}$ )/BP86/AE1//BP86/AE1 level of theory, assume that the nucleophilic reaction with CN as the electrophile occurs initially at two adjacent carbon atoms, forming a kinetic transient *vicinal*-isomer with the assumed formulation  $\{(1,2\text{-CN}_2\text{-1,2-}C_2\text{B}_9\text{H}_9)(1',2'\text{-C}_2\text{B}_9\text{H}_{11})\text{-3,3'-Co(III)}\}^-$   $\{3b^-$  (Scheme 1 and Fig. 3). The spontaneous rearrangement proceeded relatively rapidly; therefore, the presence of the transient isomer could not be reliably identified using HPLC or NMR methods. Although the CN group is an electron-withdrawing substituent towards 2D aromatics, it acts in a different way with respect to the current substitution on the  $\text{CoC}_2\text{B}_9$  “icosahedron”. Namely, the IBO charge on carbons bearing the CN groups was computed to be  $-0.22$ , a number which is not different from that detected in the parent ion by the same computational approach. The IBO HOMO/LUMO gap was computed to be only  $0.11\text{ eV}$ , which

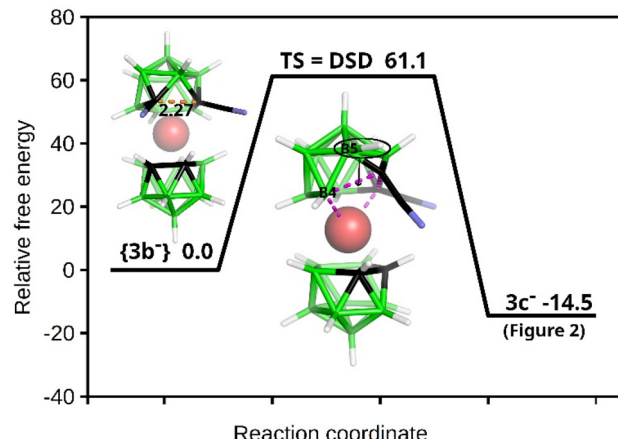


**Fig. 3** Schematic potential energy surface of the DSD-based rearrangement with the relative Gibbs free energies ( $\text{kcal mol}^{-1}$ ) as computed at the SMD( $\text{Et}_2\text{O}$ )/BP86/AE1//BP86/AE1 level of theory (for the methodology description and the Cartesian geometries of the stationary points, see Computational Details in the ESI†). The  $\text{C}(1)\text{-C}(2)$  separation in  $\{3b^-$  is given in  $\text{\AA}$ .

indicates an extreme instability of the starting 1,2-isomer of the dinitrile derivative, where the latter seemed to exist below time scaling of the NMR approach. Note that such a carbon charge in the case of its azido-substitution was  $0.00$ , which was ascribed to the electron-withdrawing abilities of the  $\text{N}_3$  group.<sup>24</sup> On that basis, transfer of electron density from the CN groups to the boron cage is apparent and causes an extreme elongation of the  $\text{C}(1)\text{-C}(2)$  nearest-neighbour separation from  $1.68\text{ \AA}$  in  $\text{Cs}^+$  salt of the parent ion<sup>29</sup> to  $2.27\text{ \AA}$  in the BP86/AE1 space of  $\{3b^-$ . Such an elongation of this distance beyond bonding limits is known from the chemistry of mixed sandwich complexes of aryl-, alkyl-, and alkane-substituted dicarbollide ligands and fragments containing transition metals of the second and third row, such as RuCp, RhCOD, and IrCOD, where the metal central unit is electron-poor, containing 16 valence electrons only, which is compensated with *semi*-open structures called *iso-closo*-, *hyper-closo*-, or *pseudo-closo*.<sup>30-33</sup> Interestingly, exceptionally long C-C nearest-neighbour separations were observed in C,C-disubstituted-*o*-carboranes; the longest for  $\text{NH}_2$  groups reached almost  $2\text{ \AA}$ .<sup>34-36</sup>

In the case of our dinitrile motif, the rearrangement process occurred in the  $\text{Co-C}(1)\text{-C}(2)\text{-B}(4)$  diamond (see Fig. 3), and the resulting isomer had an IBO HOMO/LUMO gap of  $4.44\text{ eV}$ , which seemed to be a driving force for the rearrangement. The DSD-like transition state was characterized by a strong imaginary frequency at  $-541\text{ cm}^{-1}$ . Consequently, the  $\text{B}(5)\text{-H}$  vertex, as a part of a six-membered  $\text{CB}_3$  girdle, moved to the upper four-membered  $\text{CB}_3$  girdle, which was facilitated by the positive region dictated by cobalt. In other words,  $\text{C}(1)$  and  $\text{B}(5)$  interchanged their positions after the rearrangement and two pentagonal rings were present in the resulting  $3c^-$  structure. Note that this reaction profile corresponds to the classical DSD 1,2-*closo*- $\text{C}_2\text{B}_{10}\text{H}_{10}$  to 1,7-*closo*- $\text{C}_2\text{B}_{10}\text{H}_{10}$  rearrangement computed *e.g.* in ref. 37. Note that the reaction profiles in



boron-cluster chemistry can be very complex because there exist relatively small energy differences between many intermediate and transition states. Consequently, the boron-cluster reaction may involve many competing pathways.<sup>38</sup>

Another diverse mechanism consisting in **1e**<sup>-</sup> reductive opening and oxidative closure of the cage, observed previously<sup>39</sup> for the rearrangement of the mixed sandwich [3-CpCo-1,2-C<sub>2</sub>B<sub>9</sub>H<sub>11</sub>] to a mixture of isomers inclusive of the 1,8-species apparently, does not apply in the current case, due to fact that the isomerisation to **3c** proceeded under an argon atmosphere, without the presence of any oxidation agent and in a stereospecific way.

Some analogy can be also seen with rearrangements observed previously in the case of neutral mixed Mo, W, Ru, Rh, and Ir complexes containing a dicarbollide ligand substituted with sterically demanding aryl/alkyl,<sup>40</sup> MeS, or Me<sub>2</sub>S groups<sup>41</sup> and COD or norbornadiene as the second ligand. Typically, this interconversion occurs during or inherently after metal fragment insertion into the substituted dicarbollide ligand at temperatures between 20 °C and 60 °C. Such complexes containing 2nd and 3rd-row transition metals with more diffuse f and d orbitals are inherently less stable and more prone to cage opening and isomerisation. In addition, the crowding from sterically demanding substituents on carbon atoms is an essential condition for elongating the carbon–carbon bond that gives rise to this pathway. This is, however, dissimilar to the case of the full cobalt(III) sandwich and rod-like CN groups as substituents described herein. In addition, no example of rearrangement due to post-modification of an icosahedral metallacarborane cage has yet been described, even in the mixed sandwich series.

## Conclusion

Synthetic ways to obtain carbon-substituted nitriles of the cobalt bis(dicarbollide) ion were developed. Mono- and di-substituted compounds are now available. This in turn may lead to an expanding family of various new derivatives using approaches adapted from organic chemistry, exoskeletal metal complexes, polymers, etc. The main achievement, however, consists in attaining a unique stereochemistry of the substitution *via* direct modification of the cage. It has been shown that the introduction of a particular class of substituents, in our case nitrile groups, can enable low-temperature skeletal rearrangement of carbon atoms in one dicarbollide ligand of the cobalt bis(dicarbollide) ion to the C(8) position of the cage. This was proven feasible even though the structure of ion **1**<sup>-</sup> is very robust and invulnerable towards rearrangement at temperatures up to 300 °C or higher. Based on computational support, the skeletal interconversion was determined to occur as a consequence of the entry of electron-donating CN groups sitting in vicinal carbon positions followed by a DSD mechanism, in which the Co…C(1)…C(2)…B(4) belt represents the “square” with individual next-nearest separations spanning the interval 2.1–2.7 Å (BP86/AE1). As opposed to 2D aromatics,

the CN group behaves here as an electron donor. The rearrangement proceeds in a regioselective way, and may thus offer direct access to a broad selection of other groups on ion **1**<sup>-</sup> in a geometrically unique arrangement. This may be useful for fine-tuning the interactions of the cobalt bis(dicarbollide) ion with biological targets, for the design of protein inhibitors, anticancer, antimicrobial agents, etc.

## Data availability

The data supporting of this article, consisting of the <sup>11</sup>B, <sup>1</sup>H, <sup>13</sup>C NMR spectra and HRMS results, have been included as part of the ESI.† Further, details relating to yields and signal assignments are included.

The crystallographic data for the compounds **Me<sub>4</sub>N3a** and **Me<sub>4</sub>N3c** have been deposited with the Cambridge Crystallographic Data Centre with the CCDC 2370282 and 2370281, respectively. Moreover, CheckCif files were uploaded during submission.†

## Conflicts of interest

There are no conflicts to declare.

## Acknowledgements

The authors are grateful for funding from the Czech Science Foundation Grants No. 2114409S to BG (synthesis and crystallography) and No. 23-05083S to JF (DFT computations).

## References

- 1 B. P. Dash, R. Satapathy, B. R. Swain, C. S. Mahanta, B. B. Jena and N. S. Hosmane, *J. Organomet. Chem.*, 2017, **849–850**, 170–194.
- 2 L. Pazderová, E. Z. Tüzün, D. Bavol, M. Litecká, L. Fojt and B. Grüner, *Molecules*, 2023, **28**, 67.
- 3 R. N. Grimes and R. N. Grimes, *Metallacarboranes of the Transition and Lanthanide Elements*, 2016.
- 4 J. Poater, M. Sola, C. Viñas and F. Teixidor, *Angew. Chem., Int. Ed.*, 2014, **53**, 12191–12195.
- 5 I. M. Riddlestone, A. Kraft, J. Schaefer and I. Krossing, *Angew. Chem., Int. Ed.*, 2018, **57**, 13982–14024.
- 6 V. Dordovič, Z. Tošner, M. Uchman, A. Zhigunov, M. Reza, J. Ruokolainen, G. Pramanik, P. Cíglér, K. Kalikova, M. Gradzielski and P. Matějíček, *Langmuir*, 2016, **32**, 6713–6722.
- 7 Y. Chen, A. Barba-Bon, B. Grüner, M. Winterhalter, M. A. Aksoyoglu, S. Pangeni, M. Ashjari, K. Brix, G. Salluce, Y. Folgar-Cameán, J. Montenegro and W. M. Nau, *J. Am. Chem. Soc.*, 2023, **145**, 13089–13098.
- 8 M. Gos, J. Cebula and T. M. Goszczyński, *J. Med. Chem.*, 2024, **67**, 8481–8501.



9 P. Cíglér, M. Kožísek, P. Rezáčová, J. Brynda, Z. Otwinowski, J. Pokorná, J. Plešek, B. Grűner, L. Dolečková-Marešová, M. Máša, J. Sedláček, J. Bodem, H. G. Krausslich, V. Král and J. Konvalinka, *Proc. Natl. Acad. Sci. U. S. A.*, 2005, **102**, 15394–15399.

10 M. Tarres, E. Canetta, C. Viñas, F. Teixidor and A. J. Harwood, *Chem. Commun.*, 2014, **50**, 3370–3372.

11 J. Cebula, K. Fink, J. Boratynski and T. M. Gosczynski, *Coord. Chem. Rev.*, 2023, **477**, 19.

12 C. Teixidor-Viñas, F. Teixidor and A. J. Harwood, in *Boron-Based Compounds: Potential and Emerging Applications in Medicine*, ed. E. HeyHawkins, C. Teixidor-Viñas, John Wiley & Sons Ltd, Chichester, 2018, pp. 159–173.

13 K. Fink, J. Boratynski, M. Paprocka and T. M. Gosczynski, *Ann. N. Y. Acad. Sci.*, 2019, **1457**, 128–141.

14 M. Nuez-Martinez, C. I. G. Pinto, J. F. Guerreiro, F. Mendes, F. Marques, A. Munoz-Juan, J. A. M. Xavier, A. Laromaine, V. Bitonto, N. Protti, S. G. Crich, F. Teixidor and C. Viñas, *Cancers*, 2021, **13**(24), 6367.

15 A. G. Beck-Sickinger, D. P. Becker, O. Chepurna, B. Das, S. Flieger, E. Hey-Hawkins, N. Hosmane, S. S. Jalisiati, H. Nakamura, R. Patil, M. D. H. Vicente and C. Viñas, *Cancer Biother. Radiopharm.*, 2023, **38**, 160–172.

16 E. Vařková, K. Lokočová, P. Kašparová, R. Hadravová, I. Křížová, O. Mat'atková, J. Masák and V. Šícha, *Pharmaceuticals*, 2022, **15**, 534.

17 J. Plešek, S. Heřmánek, A. Franken, I. Císařová and C. Nachtigal, *Collect. Czech. Chem. Commun.*, 1997, **62**, 47–56.

18 A. A. Druzina, A. V. Shmalko, I. B. Sivaev and V. I. Bregadze, *Russ. Chem. Rev.*, 2021, **90**, 785–830.

19 R. Núñez, I. Romero, F. Teixidor and C. Viñas, *Chem. Soc. Rev.*, 2016, **45**, 5147–5173.

20 R. Núñez, E. J. Juarez-Perez, F. Teixidor, R. Santillan, N. Farfan, A. Abreu, R. Yepez and C. Viñas, *Inorg. Chem.*, 2010, **49**, 9993–10000.

21 J. Cabrera-Gonzalez, V. Sanchez-Arderiu, C. Viñas, T. Parella, F. Teixidor and R. Núñez, *Inorg. Chem.*, 2016, **55**, 11630–11634.

22 F. Teixidor, R. Núñez and C. Viñas, *Molecules*, 2023, **28**, 24.

23 M. Kugler, J. Nekvinda, J. Holub, S. El Anwar, V. Das, V. Šícha, K. Pospíšilová, M. Fábry, V. Král, J. Brynda, V. Kašička, M. Hajdúch, P. Rezáčová and B. Grűner, *ChemBioChem*, 2021, **22**, 2741–2761.

24 Z. E. Tüzün, L. Pazderová, D. Bavol, M. Litecká, D. Hnyk, Z. Růžičková, O. Horáček, R. Kučera and B. Grűner, *Inorg. Chem.*, 2024, **4c03257**, DOI: [10.1021/acs.inorgchem.4c03257](https://doi.org/10.1021/acs.inorgchem.4c03257).

25 S. El Anwar, Z. Ružičková, D. Bavol, L. Fojt and B. Grűner, *Inorg. Chem.*, 2020, **59**, 17430–17442.

26 V. V. Volkov, G. S. Yurev, S. G. Vasileva, G. S. Voronina and K. G. Myakishev, *Bull. Acad. Sci. USSR, Chem. Sci.*, 1990, **39**, 1355–1359.

27 M. K. Kaloustian, R. J. Wiersema and M. F. Hawthorne, *J. Am. Chem. Soc.*, 1972, **94**, 6679–6686.

28 R. B. King, I. Silaghi-Dumitrescu and I. Sovago, *Inorg. Chem.*, 2009, **48**, 5088–5095.

29 A. Zalkin, T. E. Hopkins and D. H. Templeton, *Inorg. Chem.*, 1967, **6**, 1911–1915.

30 J. Bould and J. D. Kennedy, *J. Organomet. Chem.*, 2014, **749**, 163–173.

31 L. S. Alekseev, A. V. Safronov, F. M. Dolgushin, A. A. Korlyukov, I. A. Godovikov and I. T. Chizhevsky, *J. Organomet. Chem.*, 2009, **694**, 1727–1735.

32 R. M. Garrioch, G. M. Rosair and A. J. Welch, *J. Organomet. Chem.*, 2000, **614**, 153–157.

33 R. T. Baker, *Inorg. Chem.*, 1986, **25**, 109–111.

34 J. M. Oliva, N. L. Allan, P. V. Schleyer, C. Viñas and F. Teixidor, *J. Am. Chem. Soc.*, 2005, **127**, 13538–13547.

35 J. X. Li, R. L. Pang, Z. F. Li, G. Q. Lai, X. Q. Xiao and T. Müller, *Angew. Chem., Int. Ed.*, 2019, **58**, 1397–1401.

36 J. Llop, C. Viñas, J. M. Oliva, F. Teixidor, M. A. Flores, R. Kivekas and R. Sillanpää, *J. Organomet. Chem.*, 2002, **657**, 232–238.

37 B. M. Gimarc, D. S. Warren, J. J. Ott and C. Brown, *Inorg. Chem.*, 1991, **30**, 1598–1605.

38 D. Hnyk and D. A. Wann, in *Boron: The Fifth Element*, Springer, Dordrecht, 2015, vol. 20, ch. 5, pp. 17–48.

39 W. Y. Man, G. M. Rosair and A. J. Welch, *Dalton Trans.*, 2015, **44**, 15417–15419.

40 A. V. Safronov, F. M. Dolgushin, P. V. Petrovskii and I. T. Chizhevsky, *Organometallics*, 2005, **24**, 2964–2970.

41 M. M. Vinogradov, Y. V. Nelyubina, A. A. Pavlov, V. V. Novikov, N. V. Shvydkiy and A. R. Kudinov, *Organometallics*, 2017, **36**, 791–800.

